

# Effect of Th9/IL-9 on the growth of gastric cancer in nude mice

This article was published in the following Dove Medical Press journal:  
*OncoTargets and Therapy*

Li Cai<sup>1,\*</sup>  
Yue Zhang<sup>2,\*</sup>  
Yifei Zhang<sup>3</sup>  
Hongbing Chen<sup>3</sup>  
Jinchen Hu<sup>3</sup>

<sup>1</sup>Department of Pathology, The Affiliated Yantai Yuhuangding Hospital of Qingdao University, Yantai 264000, People's Republic of China;

<sup>2</sup>Department of Gastrointestinal Surgery, Laizhou People's Hospital, Yantai 264000, People's Republic of China; <sup>3</sup>Department of Gastrointestinal Surgery, The Affiliated Yantai Yuhuangding Hospital of Qingdao University, Yantai 264000, People's Republic of China

\*These authors contributed equally to this work

**Objective:** By neutralizing IL-9 in a nude mouse model, the study aimed to investigate the role of Th9/IL-9 on the growth of gastric cancer in mice.

**Materials and methods:** Male BALB/c nude mice were randomly divided into three groups: a normal control group (Control), an SGC-7901 xenografted nude mice model group (Model), and a rIL-9 treatment group (Treat). The weight of the tumors was recorded to calculate the tumor inhibition rate. Flow cytometry was used to detect the cell frequency of Th9, Th17, and Treg in peripheral blood. The IL-4, IL-9, IL-10, IL-25, VEGF, and TGF- $\beta$  levels in serum were determined by ELISA. The cellular migration and invasion were investigated by transwell assay. Immunohistochemical and Western blot were used to detect the expression of IL-9, CD34, PU.1, p53, and p21 proteins in gastric cancer tissue. The mRNA expression levels of IL-9, IL-21, and PU.1 in gastric cancer tissue were determined by qRT-PCR.

**Result:** rIL-9 can significantly inhibit the growth of gastric cancer. The frequency of Th9, Th17, and Treg in peripheral blood was decreased upon treatment. The levels of IL-4, IL-9, IL-10, IL-25, VEGF, and TGF- $\beta$  in serum were significantly reduced in the Treat group compared with the Model group ( $P < 0.05$ ). rIL-9 can inhibit cellular migration and invasion and reduce the mRNA level of IL-9, IL-21, and PU.1. Meanwhile, in the Treat group, the expression of IL-9, CD34, and PU.1 was significantly reduced, whereas the expression of p53 and p21 was significantly increased compared with the Model group ( $P < 0.05$ ).

**Conclusion:** This study suggested that Th9/IL-9 has a deleterious role in gastric cancer.

**Keywords:** Th9, IL-9, gastric cancer, CD4 T lymphocyte

## Introduction

Gastric cancer is the fourth common cancer and the second leading cause of cancer-related death worldwide.<sup>1</sup> Gastric cancer has become a significant threat to human health over the last decade.<sup>2</sup> Cytotoxicity and drug resistance were observed in the development of gastric cancer cells, which leads to tumor recurrence and even further development.<sup>3</sup> Although the progress in treatment of gastric cancer has been accelerated in recent years, the therapeutic effect is still unsatisfactory.<sup>4</sup> Therefore, it would be of great clinical value to identify new drugs or new therapeutic targets that can effectively and safely treat gastric cancer.

Accumulating data suggest that infiltrating CD4 T lymphocytes, including T helper (Th) cells and regulatory (Tregs) cells, play important roles in gastric cancer.<sup>5,6</sup> Th9 cells is a recently recognized Th cell subset, which is involved in a wide range of autoimmune diseases and allergic inflammation, and significantly regulates host response.<sup>7,8</sup> These cells exert proinflammatory or anti-inflammatory activity by modulating the development of Treg and Th17 cells.<sup>9</sup> Th9 is characterized by secreting large quantities of IL-9.<sup>10</sup> IL-9 targets cells of the lymphoid, myeloid, and mast cell lineages

Correspondence: Jinchen Hu  
Department of Gastrointestinal Surgery,  
The Affiliated Yantai Yuhuangding  
Hospital of Qingdao University, No 20  
Yuhuangding East Road, Zhufu District,  
Yantai, People's Republic of China  
Tel +860 535 669 1999  
Email chengxiaoyyy@163.com

and likely contributes to the development of autoimmune diseases.<sup>11</sup> Further research proved that IL-9 induces immunosuppression controlled by Treg and mast cells, which leads to tolerance to environmental stress.<sup>12</sup> The differentiation of Th9 cells requires balanced signaling, including IL-4, TGF- $\beta$ ,<sup>13</sup> and the epithelial cell thymic stromal lymphopoietin (TSLP),<sup>14</sup> which leads to transcription factor-induced PU.1 and interference (IFN) regulatory factor 4 (IRF4) binds directly to the IL-9 promoter and activates gene expression in Th9 cells.<sup>15</sup> Once differentiated, Th9 cells need to activate the IL-25/IL-17 RB axis to produce high levels of IL-9.<sup>16</sup> This study also showed that epigenetic modifications in the PU.1 promoter uniquely and dynamically control the threshold for Th9-cell development in naive and memory CD4 T cells and, therefore, functional maturation of the immune system.<sup>15</sup>

Given the previous research, it is reasonable to hypothesize that Th9/IL-9 may be a new therapeutic target for gastric cancer. Therefore, in this study, by neutralizing IL-9 in a nude mouse model, we describe for the first time that Th9/IL9 has a deleterious role in gastric cancer.

## Materials and methods

### Animals

Twenty-four male BALB/c nude mice (18 $\pm$ 2 g, 6–8 weeks old) were purchased from Jinan Pengyue Experimental Animal Breeding Co., Ltd. (license number SCXK (Lu) 2014-0007, Jinan, China). The mice were housed in a room under temperature 25°C $\pm$ 2°C, with a relative humidity of 55% $\pm$ 5%, 12 hour day and night alternation, and free access to water and food. All animal experiments were approved by the Institutional Animal Care Committee of The Affiliated Yantai Yuhuangding Hospital of Qingdao University and performed within the guidelines for the Care and Use of Laboratory Animals.

### Gastric cancer cell lines and cell culture

Human gastric cancer cell line SGC-7901 (TCHu 46) was obtained from American Type Culture Collection (Rockville, MD, USA). Cells were cultured in RPMI-1640 medium (HyClone, Logan, UT, USA) supplemented with 10% fetal calf serum (Gibco BRL, Grand Island, NY, USA) at 37°C under an atmosphere of 5% CO<sub>2</sub> and 95% air. Logarithmic growth-phase cells were collected for experiments.

### Experimental procedure

Male BALB/c nude mice were randomly divided into three groups, including a normal control group (Control), an SGC-7901 xenografted nude mice model group (Model),

and a rIL-9 treatment group (Treat), with 10 rats in each group. Then, 0.3 mL of single-cell suspension (1.0 $\times$ 10<sup>7</sup>/mL) in buffer solutions was injected into every mouse in the Model and Treat groups. When the tumor tissue volume reached 1 cm<sup>3</sup>, the modeling was considered successful. Then, the mice in the Treat group received 0.2 mL phosphate buffered saline (PBS) (250 ng/mL rIL-9, PeproTech, Rocky Hill, NJ, USA)<sup>17</sup> by intraperitoneal injection, while those in the Control and Model groups received an equivalent volume of PBS.

After administration once every 2 days for 28 days, the peripheral blood of each mouse was collected from mandibular venous plexus. A portion of the blood sample was centrifuged (3,500 rpm, 15 min) to yield the upper layer of serum that was collected carefully and stored at –80°C, and the remaining blood sample was placed in an anticoagulant tube for flow cytometry. Subsequently, mice were intraperitoneally injected with 1% sodium pentobarbital (40 mg/kg) and sacrificed and dissected to acquire the intact tumor tissues. The tumors were weighed to calculate the tumor inhibition rate using the following equation: Tumor growth inhibition rate (%)=(the mean tumor weight of Model group–the mean tumor weight of Treat group)/the mean tumor weight of Model group $\times$ 100%.

### The cell frequency of Th9, Th17, and Treg was detected by flow cytometry

Peripheral blood and PBS containing 1% FBS (Gibco, Grand Island, NY, USA) were used to prepare a single cell suspension. Cells were stained with FITC anti-mouse CD4 antibody (BD Bioscience PharMingen, San Jose, CA, USA) in a dark environment at 4°C for 30 minutes, and the cells were fixed and permeabilized with Cytotfix/Cytoperm buffer (BD Bioscience PharMingen). They were then stained with PE anti-mouse IL-9 or PE anti-mouse IL-17 antibody (BD Bioscience PharMingen).<sup>18</sup> To detect Tregs, cells were stained with FITC anti-mouse CD4 and APC anti-mouse CD25 (eBioscience, San Diego, CA USA), then incubated at 4°C in the dark for 20 minutes. After being washed twice, the cells were fixed, permeabilized, and stained with PE anti-mouse Foxp3 (eBioscience, USA). Flow cytometric analysis (FACSCanto II, BD Biosciences, USA) was performed, and FCS Express 4 software (De Novo Software, Glendale, CA, USA) was used for analysis.

### Inflammatory factors were detected by ELISA

The levels of IL-4 (EK0405, Boster, Pleasanton, CA, USA), IL-9 (ABIN625153, RayBiotech, Norcross, GA, USA),

IL-10 (EK0417, Boster), IL-25 (ABIN425028, Cloud-Clone, Houston, TX, USA), VEGF (ABIN2116393, antibodies-online, Germany), and TGF- $\beta$  (ABIN772539, Blue Gene, San Francisco, CA, USA) in serum were determined by ELISA kits according to the manufacturer's instructions.

### Cellular migration and invasion assay

Inserts were diluted to 20 ng/mL in RPMI 1640, then SGC-7901 cells were placed in the upper chamber of insert (Corning Inc., Corning, NY, USA) for migration assay and invasion assay, and the SGC-7901 cells were placed in the upper chamber of inserts coated with 45  $\mu$ g of Matrigel (BD Biosciences) for invasion assay. Six hundred microliters of complete medium containing 10% FBS was added to the lower layer of Transwell (MilliporeSigma, Burlington, MA, USA) 24-well plate and incubated at 37°C in 5% CO<sub>2</sub> for 24 hours. Next, the cells attached to the lower surface were stained with crystal violet at room temperature for 20 minutes. Then, the plates were rinsed with PBS, and the number of cells on the membrane were counted manually using an inverted microscope (Olympus, Tokyo, Japan).

### The expression of IL-9 and CD34 were detected by immunohistochemistry

The tumors in each group were embedded in paraffin, sliced, and dewaxed into the water. Then, the tumors were inactivated with methanol (3% H<sub>2</sub>O<sub>2</sub>) for 20 minutes, repaired in citrate buffer (pH 6.0) for 10 minutes, and blocked in 5% BSA for 20 minutes. The tumors were incubated overnight at 4°C with rabbit anti-mouse IL-9 (1:100, ab203386, Abcam, Cambridge, MA, USA) and hematopoietic progenitor cell antigen CD34 (CD34) (1:1,000, ABIN1111107, antibodies-online, Aachen, Germany) antibody, respectively. Subsequently, horseradish peroxidase-labeled goat anti-rabbit IgG (ABIN101988, antibodies-online, Germany) was used. DAB coloration, counterstaining, dehydration, clearing, and mounting followed (Fisher Scientific, Ottawa, ON, Canada). The expression of IL-9 was observed by Mirax Scan (Zeiss, Don Mills, ON, Canada), counted by AperioImageScope 11.1 software, and the results were expressed as positive cells/mm<sup>2</sup>.

### The expressions of related mRNAs were detected by reverse transcription-polymerase chain reaction (RT-PCR)

The tumor tissue was collected and TRIzol reagent (Invitrogen, Carlsbad, CA, USA) was used for RNA extraction. The reverse transcription procedure was per-

formed according to the instructions of the kit (Applied Biosystems, Waltham, MA, USA). qRT-PCR amplification was performed using the Mastercycler<sup>®</sup> nexus X2 (Eppendorf, Hamburg, Germany). The following primers were used: 5'-AACAGTCCCTCCCTGTAGCA-3' (forward) and 5'-AAGGATGATCCACCGTCAAA-3' (reverse) for IL-9, 5'-AAAACAGGCAAAGCTGCAT-3' (forward) and 5'-TGACATTGTTGAACAGCTGAAA-3' (reverse) for IL-21, 5'-AGGAGTCTTCTACGACCTGGA-3' (forward) and 5'-GAAGGCTTCATAGGGAGCGAT-3' (reverse) for PU.1, and 5'-CGTCATTGCACGAAGACACAA-3' (forward) and 5'-CCTGGTCCACCATTTTAAGGC-3' (reverse) for  $\beta$ -actin. Reaction conditions were as follow: 95°C for 120 seconds, followed by 95°C for 15 seconds, then 60°C for 15 seconds, and repeated for 40 cycles. The expression levels of the gene mRNA were calculated by the 2<sup>- $\Delta\Delta$ CT</sup> method and  $\beta$ -actin was used as the endogenous control.

### The expressions of related proteins were detected by Western blot

Tissues were homogenized after grinding. Then, centrifugation was performed at 2,000 r/min for 20 minutes at 4°C. After being quantitated with the bicinchoninic acid (BCA) protein assay kit (Pierce, Rockford, IL, USA), proteins were separated by 10% SDS-PAGE and transferred onto polyvinylidene difluoride (PVDF) membrane (Millipore, USA). The membranes were blocked with 5% skim milk for 1 hour at room temperature. Then, the membranes were incubated overnight at 4°C with primary antibodies against PU.1 (1:1,000, sc-390659, Santa Cruz, CA, USA), P53 (1:1,000, ABIN1499973, antibodies-online, Aachen, Germany), P21 (1:1,000, ABIN2855705, antibodies-online), and  $\beta$ -actin (1:1,000, ABIN2854709, antibodies-online). Subsequently, secondary antibody IgG-HRP (1:1,000, #7074, Cell Signaling Technology, Danvers, MA, USA) was used and incubated for 0.5 hour at room temperature. The blots were visualized with enhanced chemiluminescence (ECL) system (ImageQuant LAS 4000, General Electric Company, Fairfield, CT, USA), and the results were analyzed by LabImage version 2.7.1 (Kapelan GmbH, Halle, Germany).

### Statistical analysis

Statistical analysis was performed using SPSS 19.0 (SPSS Inc., Chicago, IL). Data are reported as the mean value $\pm$ SD ( $\bar{x}\pm$ SD). Significant differences between two groups were assessed by *t*-test, one-way ANOVA was used for multi-group data analysis, and LSD test was used for subsequent analysis. *P*<0.05 was considered statistically significant.

## Results

### rIL-9 inhibited the tumor growth in SGC-7901-xenografted nude mice

Tumors grew at the site of inoculation after being inoculated for 6–9 days. The tumor formation rate was 100%, and no spontaneous tumor regression was observed. As displayed in Figure 1, compared with the Model group, the growth of tumors in the Treat group was significantly slower on the 14th day of rIL-9 treatment (from  $300.5 \pm 55.7 \text{ mm}^3$  to  $196.8 \pm 37.6 \text{ mm}^3$ ,  $P < 0.05$ ). On the 28th day, the tumor volume and average tumor weight in the Treat group were significantly reduced (both  $P < 0.05$ ). After rIL-9 treatment, the tumor growth inhibition rate was 64.8%.

### rIL-9 inhibited the cell frequency of Th9, Th17, and Treg in peripheral blood of SGC-7901-xenografted nude mice

As shown in Figure 2, the cell frequency of Th9, Th17, and Treg in the Model group was  $1.68 \pm 0.20$ ,  $6.67 \pm 0.65$ , and  $10.61 \pm 1.20$ , respectively; this was significantly higher compared to the Control group ( $P < 0.05$ ). However,

the use of rIL-9 significantly reduced the cell frequency of Th9, Th17, and Treg in peripheral blood of SGC-7901-xenografted nude mice ( $0.68 \pm 0.12$ ,  $2.69 \pm 0.36$ , and  $5.64 \pm 0.49$ , respectively). The results indicated that rIL-9 inhibited the cell frequency of Th9, Th17, and Treg in peripheral blood of SGC-7901-xenografted nude mice.

### rIL-9 inhibited the factors in the serum of SGC-7901-xenografted nude mice

Compared with the Control group, the levels of IL-4, IL-9, IL-10, IL-25, VEGF, and TGF- $\beta$  in the Model group were significantly increased (from  $19.45 \pm 2.32$  to  $56.59 \pm 5.79$  for IL-4, from  $27.73 \pm 5.73$  to  $79.64 \pm 6.04$  for IL-9, from  $12.49 \pm 2.98$  to  $48.87 \pm 5.81$  for IL-10, from  $10.57 \pm 1.71$  to  $72.70 \pm 4.42$  for IL-25, from  $205.65 \pm 15.60$  to  $754.68 \pm 34.02$  for VEGF, and from  $217.42 \pm 19.84$  to  $362.93 \pm 31.50$  for TGF- $\beta$ , respectively,  $P < 0.05$ ). The treatment of rIL-9 significantly reduced the levels of those factors in the serum of SGC-7901-xenografted nude mice (Figure 3). The results showed that rIL-9 can reduce the inflammatory factors and tumor cell-induced angiogenesis and metastasis in the murine model.

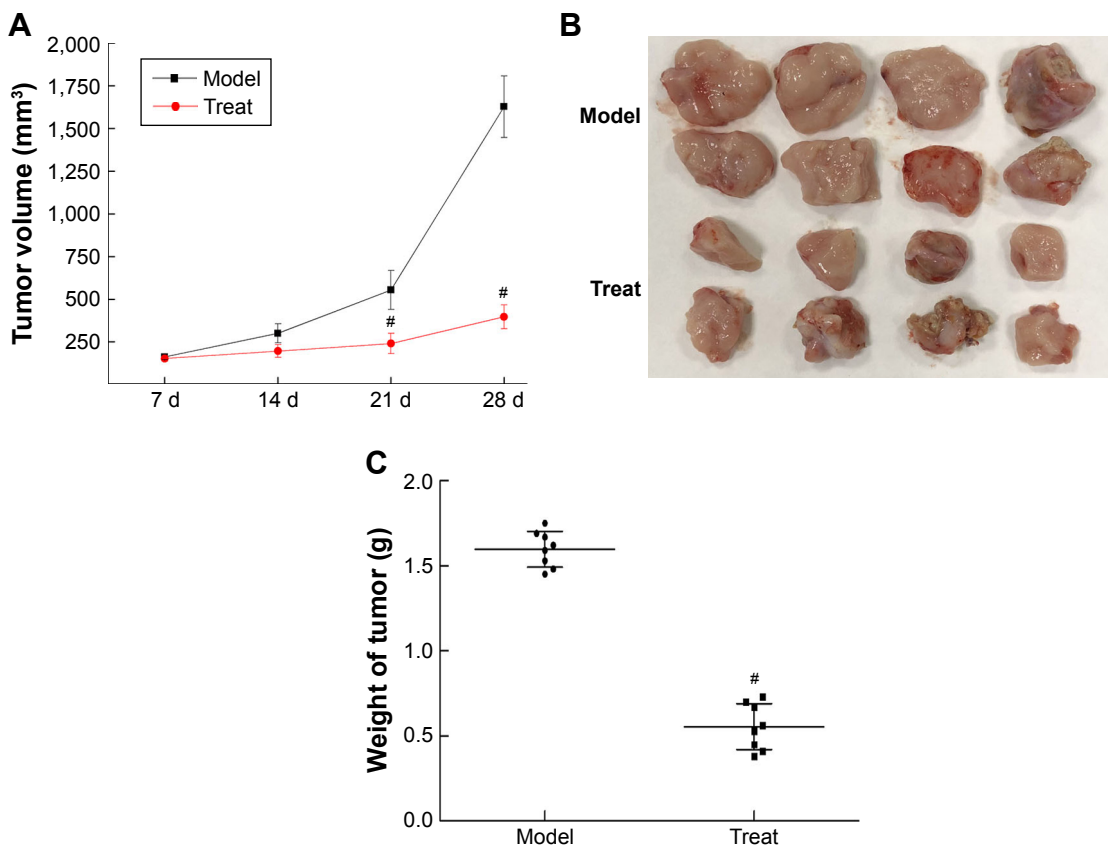


**Figure 1** Effect of rIL-9 on tumor growth in SGC-7901-xenografted nude mice, rIL-9 inhibited the tumor volume (**A**, **B**) and average tumor weight (**C**) in SGC-7901-xenografted nude mice. Data were shown as mean $\pm$ SD. # $P < 0.05$  vs model group.

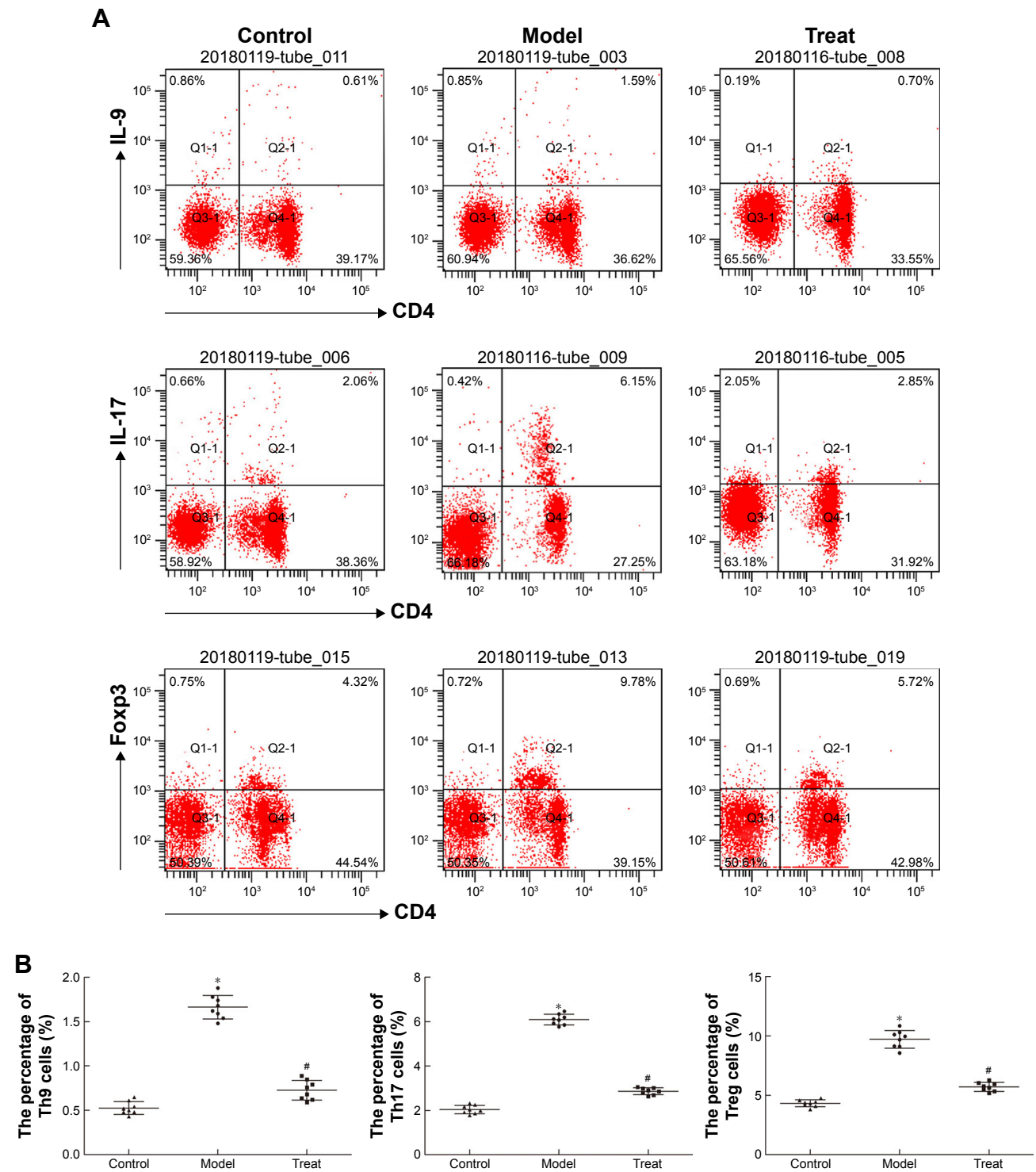


**Figure 2** Effect of rIL-9 on the cell frequency of Th9, Th17, and Treg in peripheral blood of SGC-7901-xenografted nude mice (A). rIL-9 inhibited the cell frequency of Th9, Th17, and Treg in peripheral blood of SGC-7901-xenografted nude mice (B).  
**Notes:** Data are shown as mean±SD. \*P<0.05 vs Control group, #P<0.05 vs Model group.

### rIL-9 inhibited the migration and invasion of the SGC-7901 cells

As shown in Figure 4, compared with the Control group, the migration and invasion ability of the gastric cancer cells in the

Model group was significantly increased (from 80.09±5.82 to 179.12±9.55 for relative cell migration number and from 51.63±4.17 to 144.04±13.2 for relative cell invasion number, P<0.05). However, the migration and invasion ability of

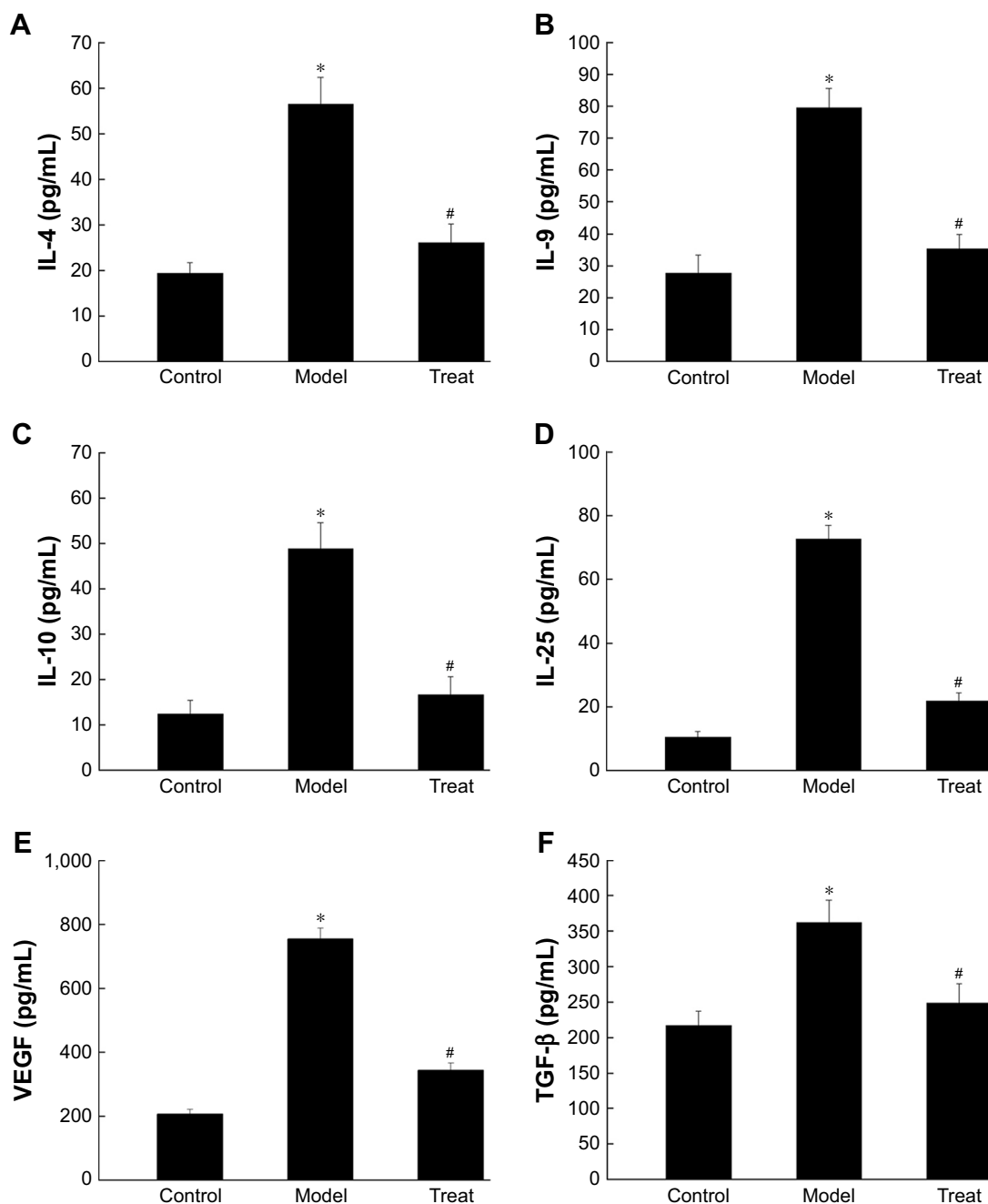


**Figure 3** Effect of rIL-9 on the factors in serum of SGC-7901-xenografted nude mice. rIL-9 could inhibit the levels of IL-4 (A), IL-9 (B), IL-10 (C), IL-25 (D), VEGF (E), and TGF-β (F) in serum of SGC-7901-xenografted nude mice.

**Notes:** Data are shown as mean±SD. \* $P < 0.05$  vs Control group, # $P < 0.05$  vs Model group.

the gastric cancer cells in the Treat group were significantly decreased ( $P < 0.05$ ). These results indicated that IL-9 can promote tumor migration and invasion, and rIL-9 could effectively inhibit the metastasis of gastric cancer cells.

### rIL-9 inhibited the expression of IL-9 and CD34 in gastric cancer tissue

CD34 is a transmembrane glycoprotein grouped into the CD34 family. It is found in hematopoietic stem cells in the vascular

endothelium of small vessels in a few neoplastic cell lines.<sup>19</sup> As shown in Figure 5, the CD34 markers in the blood vessels with cytoplasmic and/or membrane labeling were observed, and the expression of IL-9 and CD34 proteins in the Model group was positive. After treatment with rIL-9, the blood vessels with cytoplasmic and/or membrane labeling were increased, and the expression of IL-9 and CD34 proteins in the Treat group was significantly reduced ( $P < 0.05$ ). This result showed that rIL-9 has a significant inhibitory effect on tumor growth.

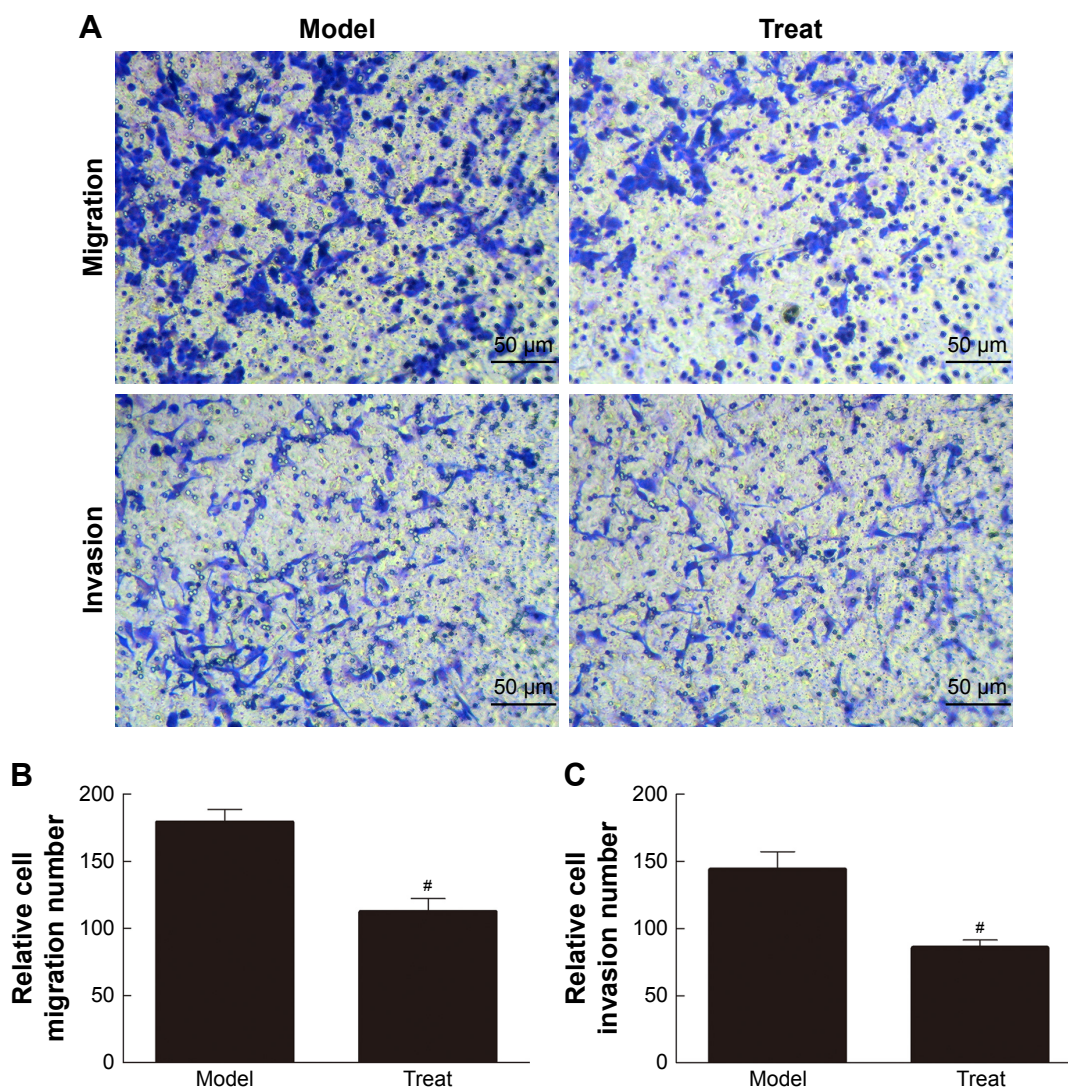


**Figure 4** Effect of rIL-9 on the migration and invasion of SGC-7901 cell (A). IL-9 can promote tumor migration (B) and invasion (C) (400×). Data were shown as mean±SD. <sup>#</sup> $P < 0.05$  vs model group.

## rIL-9 inhibited the mRNA expression of IL-9, IL-21, and PU.1 in gastric cancer tissue

As shown in Figure 6, after treatment with rIL-9, the relative mRNA levels of IL-9, IL-21, and PU.1 in the Treat group were significantly lower than those in the Model group (from  $4.15 \pm 0.62$  to  $1.23 \pm 0.32$  for IL-9, from  $5.15 \pm 0.45$  to  $1.15 \pm 0.13$  for IL-21, and from  $3.77 \pm 0.34$  to  $1.32 \pm 0.28$  for PU.1,  $P < 0.05$ , respectively). These results indicated that rIL-9 could inhibit the mRNA expression of IL-9, IL-21, and PU.1 in gastric cancer tissue.

## The expression of PU.1, p53, and p21 proteins in gastric cancer tissue

Western blot was used to detect the expression of PU.1, p53, and p21 proteins in gastric cancer tissue (Figure 7). In the Treat

group, the expression of PU.1 was significantly reduced, whereas the expression of p53 and p21 was significantly increased compared with the Control group ( $P < 0.05$ , respectively).

## Discussion

Accumulating evidence suggests that several CD4<sup>+</sup> Th subsets and their cytokines play crucial roles in the pathogenesis of tumor immunity.<sup>20</sup> The differentiation of T cells into Th subsets such as Th9, Th17, and Treg is largely dependent on the microenvironment composed of secreted cytokines. There might be a complex regulatory network between Th9, Th17, and Treg, and a positive correlation among Th9, Th17, and Treg cells was shown by Nowak and Noelle<sup>21</sup> and Stephens et al.<sup>22</sup> In our study, we found a positive correlation among Th9, Th17, and Treg frequencies in peripheral blood of

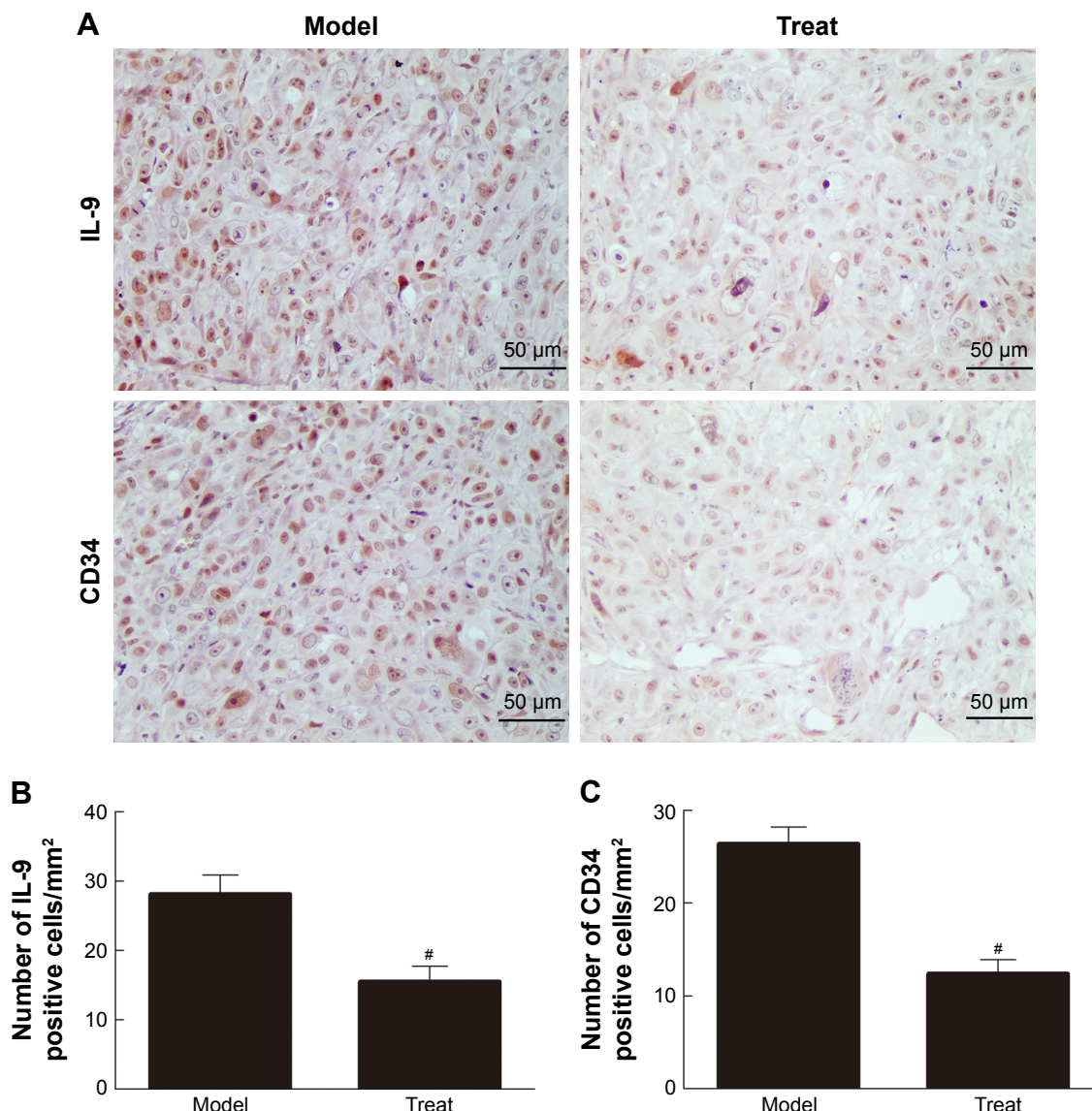


**Figure 5** Effect of rIL-9 on the expression of IL-9 and CD34 proteins in gastric cancer tissue (A). rIL-9 could inhibit the expression of IL-9 (B) and CD34 (C). Notes: Data are shown as mean±SD. <sup>#</sup>P<0.05 vs Model group.

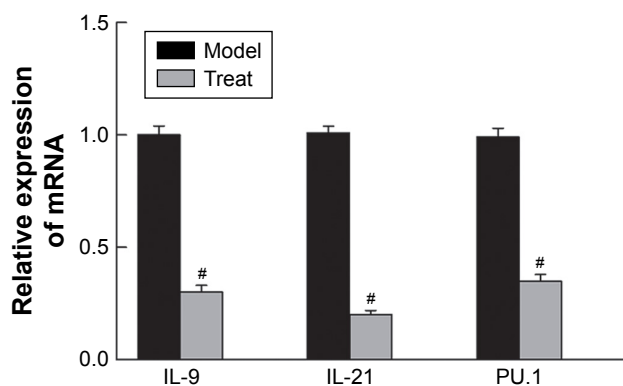


**Figure 6** Effect of rIL-9 on the mRNA expression of IL-9, IL-21, and PU.1 in gastric cancer tissue. rIL-9 can inhibit the mRNA expression of IL-9, IL-21, and PU.1. Notes: Data are shown as mean±SD. <sup>#</sup>P<0.05 vs Model group.

SGC-7901-xenografted nude mice. These results proved that the microenvironment by gastric cancer favors Th9 proliferation and IL-9 secretion. IL-21 is secreted by activated CD4+ T cells, and its receptor is expressed on many immune cells. IL-21 has an important regulating effect on the immune cells and has been linked to autoimmune diseases, allergies, and other inflammatory diseases.<sup>23</sup> Previous studies have shown that IL-21 has an important role in Th9 differentiation.<sup>24,25</sup> In this study, the use of rIL-9 suppressed the cell frequency of Th9, Th17, and Treg in peripheral blood and inhibited the mRNA expression of IL-9 and IL-21 in gastric cancer tissue. Furthermore, cellular migration and invasion and the levels of inflammatory cytokines were inhibited with the use of rIL-9.



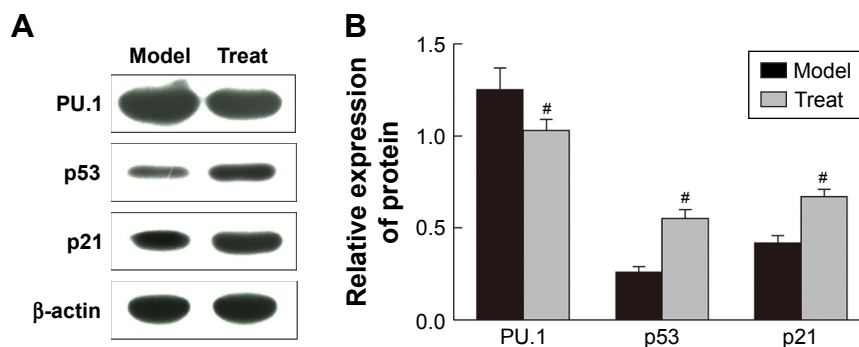


**Figure 7** Effect of rIL-9 on the expression of PU.1, p53, and p21 proteins in gastric cancer tissue (**A**). rIL-9 can reduce the expression of PU.1 and increase the expression of p53 and p21 (**B**).

**Notes:** Data are shown as mean±SD. <sup>#</sup>*P*<0.05 vs Model group.

The results show that rIL-9 has a significant inhibitory effect on tumor growth.

Energy availability supplied by neo-angiogenesis is one of the mechanisms to control cancer cells.<sup>26</sup> If neo-angiogenesis is under control, the tumor size and progression of malignancy will be under control as well.<sup>27</sup> The pathogenesis and progression of cancer are largely due to VEGF and its signaling pathway.<sup>28</sup> These results demonstrated that treatment of rIL-9 significantly reduced the level of VEGF in the serum of SGC-7901-xenografted nude mice, which illustrated that rIL-9 can reduce tumor cell-induced angiogenesis and metastasis in a murine model.

PU.1 is an ETS family transcription factor, which is critical for Th9 cell differentiation.<sup>29</sup> Th9 cell differentiation is controlled by unique and dynamic epigenetic modifications in its promoter region, and PU.1 is the master transcription factor of Th9-cell differentiation.<sup>30</sup> PU.1 enhances gene transcription through recruiting histone acetyltransferases (HATs) and enhancing permissive chromatin structure, and therefore control the functional maturation of the immune system.<sup>31</sup> P53 and p21 are tumor suppressor proteins that regulate the expression of a wide variety of genes, including apoptosis, growth inhibition, inhibition of cell cycle progression, differentiation, and accelerated DNA repair.<sup>32</sup> Previous study demonstrated that PU.1 could reduce the transcriptional activity of the p53 tumor suppressor family and, thus, inhibit activation of genes important for cell cycle regulation and apoptosis.<sup>33</sup> In our study, rIL-9 can inhibit the mRNA and protein expression of PU.1, whereas it can promote the expression of p53 and p21 proteins in gastric cancer tissue.

## Conclusion

In summary, our results demonstrate that rIL-9 can suppress cancer-related inflammatory factors, proteins, and mRNAs

in nude mice and reduce tumor cell-induced angiogenesis and metastasis. Our study suggested that Th9/IL-9 has a deleterious role in gastric cancer.

## Acknowledgment

This research received no specific grant from any funding agency in the public, commercial, or not-for-profit sectors.

## Disclosure

The authors declare no conflicts of interest in this work.

## References

1. Siegel R, Ma J, Zou Z, Jemal A. Cancer statistics, 2014. *CA Cancer J Clin*. 2014;64(1):9–29. doi:10.3322/caac.21208
2. Elimova E, Shiozaki H, Wadhwa R, et al. Medical management of gastric cancer: a 2014 update. *World J Gastroenterol*. 2014;20(38):13637–13647. doi:10.3748/wjg.v20.i38.13637
3. Tsutani Y, Yoshida K, Sanada Y, et al. Decreased orotate phosphoribosyltransferase activity produces 5-fluorouracil resistance in a human gastric cancer cell line. *Oncol Rep*. 2008;20(6):1545–1551.
4. Sakuramoto S, Sasako M, Yamaguchi T, et al. ACTS-GC Group Adjuvant chemotherapy for gastric cancer with S-1, an oral fluoropyrimidine. *N Engl J Med*. 2007;357(18):1810–1820. doi:10.1056/NEJMoa072252
5. Huang D, Yang Y, Zhang S, et al. Regulatory T-cell density and cytotoxic T lymphocyte density are associated with complete response to neoadjuvant paclitaxel and carboplatin chemoradiotherapy in gastric cancer. *Exp Ther Med*. 2018;16(5):3813–3820. doi:10.3892/etm.2018.6684
6. Tada Y, Togashi Y, Kotani D, et al. Targeting VEGFR2 with Ramucirumab strongly impacts effector/activated regulatory T cells and CD8+ T cells in the tumor microenvironment. *J Immunother Cancer*. 2018;6(1):106. doi:10.1186/s40425-018-0403-1
7. Niu Y, Liu H, Yin D, et al. The balance between intrahepatic IL-17(+) T cells and Foxp3(+) regulatory T cells plays an important role in HBV-related end-stage liver disease. *BMC Immunol*. 2011;12:47. doi:10.1186/1471-2172-12-47
8. Mucida D, Cheroutre H. The many face-lifts of CD4 T helper cells. *Adv Immunol*. 2010;107:139–152. doi:10.1016/B978-0-12-381300-8.00005-8
9. Li H, Rostami A. IL-9: basic biology, signaling pathways in CD4+ T cells and implications for autoimmunity. *J Neuroimmune Pharmacol*. 2010;5(2):198–209. doi:10.1007/s11481-009-9186-y

10. Jiang S, Wang Z, Ouyang H, Liu Z, Li L, Shi Y. Aberrant expression of cytokine interleukin 9 along with interleukin 4 and interferon gamma in connective tissue disease-associated interstitial lung disease: association with severity of pulmonary fibrosis. *Arch Med Sci*. 2016;12(1):101–106. doi:10.5114/aoms.2015.47877
11. Ouyang H, Shi Y, Liu Z, et al. Increased interleukin-9 and CD4+ IL-9+ T cells in patients with systemic lupus erythematosus. *Mol Med Rep*. 2013;7(3):1301–1307. doi:10.3892/mmr.2013.1258
12. Smith SE, Hoelzinger DB, Dominguez AL, Van Snick J, Lustgarten J. Signals through 4-1BB inhibit T regulatory cells by blocking IL-9 production enhancing antitumor responses. *Cancer Immunol Immunother*. 2011;60(12):1775–1787. doi:10.1007/s00262-011-1075-6
13. Kaplan MH, Hufford MM, Olson MR. The development and in vivo function of T helper 9 cells. *Nat Rev Immunol*. 2015;15(5):295–307. doi:10.1038/nri3824
14. Yao W, Zhang Y, Jabeen R, et al. Interleukin-9 is required for allergic airway inflammation mediated by the cytokine TSLP. *Immunity*. 2013;38(2):360–372. doi:10.1016/j.immuni.2013.01.007
15. Ramming A, Druzd D, Leipe J, Schulze-Koops H, Skapenko A. Maturation-related histone modifications in the PU.1 promoter regulate Th9-cell development. *Blood*. 2012;119(20):4665–4674. doi:10.1182/blood-2011-11-392589
16. Angkasekwinai P, Srimanote P, Wang YH, et al. Interleukin-25 (IL-25) promotes efficient protective immunity against *Trichinella spiralis* infection by enhancing the antigen-specific IL-9 response. *Infect Immun*. 2013;81(10):3731–3741. doi:10.1128/IAI.00646-13
17. Hoelzinger DB, Dominguez AL, Cohen PA, Gendler SJ. Inhibition of adaptive immunity by IL-9 can be disrupted to achieve rapid T cell sensitization and rejection of progressive tumor challenges. *Cancer Res*. 2014;74(23):6845–6855. doi:10.1158/0008-5472.CAN-14-0836
18. Liang J, Zhang B, Shen RW, et al. The effect of antifibrotic drug halofuginone on Th17 cells in concanavalin A-induced liver fibrosis. *Scand J Immunol*. 2014;79(3):163–172. doi:10.1111/sji.12144
19. Gonçalves PGP, Lourenço SIM, de Vasconcelos Gurgel BC. Immunohistochemical study of CD34 and podoplanin in periodontal disease. *J Periodontol Res*. 2019. doi:10.1111/jre.12635
20. Moeller J, Hültner L, Schmitt E, Breuer M, Dörmer P. Purification of MEA, a mast cell growth-enhancing activity, to apparent homogeneity and its partial amino acid sequencing. *J Immunol*. 1990;144(11):4231–4234.
21. Nowak EC, Noelle RJ. Interleukin-9 as a T helper type 17 cytokine. *Immunology*. 2010;131(2):169–173. doi:10.1111/j.1365-2567.2010.03332.x
22. Stephens GL, Swerdlow B, Benjamin E, et al. IL-9 is a Th17-derived cytokine that limits pathogenic activity in organ-specific autoimmune disease. *Eur J Immunol*. 2011;41(4):952–962. doi:10.1002/eji.201040879
23. Davis MR, Zhu Z, Hansen DM, Bai Q, Fang Y. The role of IL-21 in immunity and cancer. *Cancer Lett*. 2015;358(2):107–114. doi:10.1016/j.canlet.2014.12.047
24. You FP, Zhang J, Cui T, et al. Th9 cells promote antitumor immunity via IL-9 and IL-21 and demonstrate atypical cytokine expression in breast cancer. *Int Immunopharmacol*. 2017;52:163–167. doi:10.1016/j.intimp.2017.08.031
25. Liao W, Spolski R, Li P, et al. Opposing actions of IL-2 and IL-21 on Th9 differentiation correlate with their differential regulation of BCL6 expression. *Proc Natl Acad Sci U S A*. 2014;111(9):3508–3513. doi:10.1073/pnas.1301138111
26. Kopeć M, Abramczyk H. Angiogenesis—a crucial step in breast cancer growth, progression and dissemination by Raman imaging. *Spectrochim Acta A Mol Biomol Spectrosc*. 2018;198:338–345. doi:10.1016/j.saa.2018.02.058
27. Liang H, Xiao J, Zhou Z. Hypoxia induces miR-153 through the IRE1 $\alpha$ -XBP1 pathway to fine tune the HIF1 $\alpha$ /VEGFA axis in breast cancer angiogenesis. *Oncogene*. 2018;37(15):1961–1975. doi:10.1038/s41388-017-0089-8
28. Sohn EJ, Jung DB, Lee H, et al. CNOT2 promotes proliferation and angiogenesis via VEGF signaling in MDA-MB-231 breast cancer cells. *Cancer Lett*. 2018;412:88–98. doi:10.1016/j.canlet.2017.09.052
29. Chang HC, Zhang S, Thieu VT, et al. PU.1 expression delineates heterogeneity in primary Th2 cells. *Immunity*. 2005;22(6):693–703. doi:10.1016/j.immuni.2005.03.016
30. Chang HC, Sehra S, Goswami R, et al. The transcription factor PU.1 is required for the development of IL-9-producing T cells and allergic inflammation. *Nat Immunol*. 2010;11(6):527–534. doi:10.1038/ni.1867
31. Goswami R, Kaplan MH. Gcn5 is required for PU.1-dependent IL-9 induction in Th9 cells. *J Immunol*. 2012;189:3026–3033. doi:10.4049/jimmunol.1201496
32. Fujino T, Yokokawa R, Oshima T, Hayakawa M. SIRT1 knockdown up-regulates p53 and p21/Cip1 expression in renal adenocarcinoma cells but not in normal renal-derived cells in a deacetylase-independent manner. *J Toxicol Sci*. 2018;43(12):711–715. doi:10.2131/jts.43.711
33. Tschan MP, Reddy VA, Ress A, Arvidsson G, Fey MF, Torbett BE. Binding to the p53 family of tumor suppressors impairs their transcriptional activity. *Oncogene*. 2008;27(24):3489–3493. doi:10.1038/sj.onc.1211004

## OncoTargets and Therapy

### Publish your work in this journal

OncoTargets and Therapy is an international, peer-reviewed, open access journal focusing on the pathological basis of all cancers, potential targets for therapy and treatment protocols employed to improve the management of cancer patients. The journal also focuses on the impact of management programs and new therapeutic agents and protocols on

Submit your manuscript here: <http://www.dovepress.com/oncotargets-and-therapy-journal>

Dovepress

patient perspectives such as quality of life, adherence and satisfaction. The manuscript management system is completely online and includes a very quick and fair peer-review system, which is all easy to use. Visit <http://www.dovepress.com/testimonials.php> to read real quotes from published authors.